NANO LETTERS

Letter

pubs.acs.org/NanoLett

Experimental-Computational Study of Shear Interactions within Double-Walled Carbon Nanotube Bundles

Tobin Filleter,[†] Scott Yockel,[‡] Mohammad Naraghi,[†] Jeffrey T. Paci,[‡,§] Owen C. Compton,[‡] Maricris L. Mayes,[‡] SonBinh T. Nguyen,[‡] George C. Schatz,[‡] and Horacio D. Espinosa[†,*]

[†]Department of Mechanical Engineering, Northwestern University, 2145 Sheridan Road, Evanston, Illinois 60208-3111, United States

[‡]Department of Chemistry, Northwestern University, Evanston, Illinois 60208-3113, United States

[§]Department of Chemistry, University of Victoria, British Columbia, Canada V8W 3V6

Supporting Information

ABSTRACT: The mechanical behavior of carbon nanotube (CNT)-based fibers and nanocomposites depends intimately on the shear interactions between adjacent tubes. We have applied an experimental-computational approach to investigate the shear interactions between adjacent CNTs within individual double-walled nanotube (DWNT) bundles. The force required to pull out an inner bundle of DWNTs from an outer shell of DWNTs was measured using in situ scanning electron microscopy methods. The normalized force per CNT−CNT interaction (1.7 ± 1.0 nN) was found to be considerably higher than molecular mechanics (MM)-based predictions for bare CNTs (0.3 nN). This MM result is similar to the force that results from exposure of newly formed CNT surfaces, indicating that the observed pullout force arises from factors beyond what arise from potential energy effects associated with bare CNTs. Through further theoretical considerations we show that the experimentally measured pullout force may include small contributions from carbonyl functional groups terminating the free ends of the CNTs, corrugation of the CNT−CNT interactions, and polygonization of the nanotubes due to their mutual interactions. In addition, surface functional groups, such as hydroxyl groups, that may exist between the nanotubes are found to play an unimportant role. All of these potential energy effects account for less than half of the ~1.7 nN force. However, partially pulled-out inner bundles are found not to pull back into the outer shell after the outer shell is broken, suggesting that dissipation is responsible for more than half of the pullout force. The sum of force contributions from potential energy and dissipation effects are found to agree with the experimental pullout force within the experimental error.

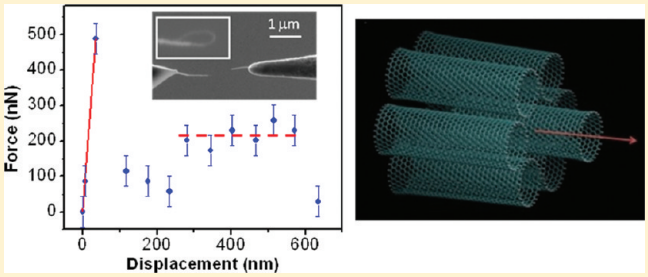

KEYWORDS: *Carbon nanotube bundles, double-walled nanotubes, hierarchical structure, shear interactions, in situ SEM testing*

Experiments and simulations targeting the mechanical behavior of carbon nanotubes (CNTs) point to modulus, strength, and toughness values of approximately 1 TPa, 100 GPa, and 3000 J/g, respectively.[1−4] Therefore, CNTs have been considered for use as building blocks and reinforcement elements to improve the mechanical behavior of nanocomposites and yarns.[5−9] In addition to their remarkable mechanical properties, CNTs have high thermal stability and tunable electrical properties, which can be exploited to develop multifunctional nanocomposites.[10,11] Despite their many advantages as nanomaterial building blocks, the realization of optimal mechanical behavior of CNTs at the macroscopic scale remains elusive.[9] This is predominantly due to weak shear interactions between CNTs, and their mutual sliding at low stress compared to their intrinsic strength, a phenomenon which does not allow for stress to build up in the tubes prior to macroscopic failure of the bulk material.[12]

Several approaches have been devised and implemented to enhance the shear interactions between CNTs and CNT shells, including electron beam (e-beam)-induced cross-linking of shells, and functionalization of CNTs in nanocomposites. In e-beam-induced cross-linking, exposure of multiwalled nanotubes (MWNTs) to radiation by high energy electrons is used to covalently cross-link adjacent shells, allowing a higher fraction of load transfer from outer to inner shells, thus increasing the load-bearing cross section of the CNTs and their effective mechanical properties. Similarly, in a bundle of CNTs, the tubes in the outer layers can be covalently cross-linked to the inner tubes, resulting in increased effective mechanical properties. By adjusting the dose of e-beam radiation, the shear interaction between CNT shells can be made very strong, such that CNT loading results in the failure of all the shells with no discernible mutual sliding.[1,13] However, e-beam cross-linking has several disadvantages; it inherently introduces defects in the CNTs that reduce the strength and modulus of individual shells,[1,14,15] and it only allows for covalent cross-links

Received: October 19, 2011
Revised: December 20, 2011
Published: January 3, 2012

   dx.doi.org/10.1021/nl203686d | *Nano Lett.* 2012, 12, 732−742

between CNT shells, leading to stiff structures, and thus only minimal energy dissipation during sliding. Alternatively, the surface of CNTs can be chemically functionalized; this method has primarily been applied to form chemical bonds with polymer matrices in nanocomposites where the polymer molecules transfer load between CNTs.[9,11,16−18] We have recently demonstrated that by using this latter approach, polymer intermediaries can be used to form compliant junctions between adjacent double-walled nanotube (DWNT) bundles within CNT yarns, which get stretched and store/dissipate energy during mechanical deformation and mutual sliding of the tubes.[12] While the incorporation of polymer intermediaries between adjacent bundles has led to significant enhancements in energy-to-failure in particular, the nature of shear interactions within the DWNT bundles remains to be further understood.

Herein we report an experimental-computational approach to investigate the shear interactions within bundles of chemical vapor deposition (CVD)-grown DWNTs. Nanomechanical tension experiments have been applied to individual bundles which can be divided into two phases. In the first phase, the bundle, which is gripped on its outside layer, is loaded axially. This phase continues until the outer layer of CNTs fails. In the second phase, the interior CNTs are pulled out of the outer layer. The first phase is mainly dominated by the tensile strength of the outer layer of CNTs, while the second phase is dominated by the shear interactions between tubes within the bundle. In this work, we have focused on investigating the second phase. A quantitative understanding of such shear interactions has not been adequately addressed in the literature even though these interactions play a key role in the resulting mechanical properties of CNT yarns. The high strength of CNT fibers spun directly from CVD processes has previously been attributed to van der Waals (vdW) interactions between adjacent CNTs within the fibers.[19,20] However, direct evidence at the individual CNT or bundle level has not yet been demonstrated.

Shear interactions within multiwalled carbon nanotubes (MWNTs) have been previously experimentally investigated.[21,22] The force necessary to extract an inner tube from a MWNT was found to be predominantly due to the vdW energy necessary to create new surface, and only negligible dissipation was observed.[21] In the context of CNT-based yarns, this previous work involved probing the forces that act at the lowest level of hierarchy, between adjacent graphitic layers within individual MWNTs. Here, we study the pullout forces and dissipation in CNT bundles, the next level in the hierarchy.

Qian et al[23] previously investigated the shear interaction between single-walled CNTs (SWNTs) within bundles by examining the force necessary to extract the inner tube from a hexagonal close-packed bundle of seven SWNTs. They estimated the extraction forces using a Lennard-Jones-based force field, and their analysis suggested that the shear interactions between tubes could be divided into two parts: (1) a contribution from the corrugation force resulting from the energy cost associated with moving atoms in and out of vdW registry with those on adjacent tubes and (2) a force due to the energy necessary to create new surfaces. The former, they suggested, is a function of the overlap length, and the latter is not. The latter is due to an increase in energy that occurs due to the creation of newly exposed surface, which previously had dispersive interactions with its neighbors. Furthermore, such interactions are larger than would be the case if the tubes were rigid, because adjacent tubes flatten somewhat against their neighbors.[24] This effect has recently been directly confirmed experimentally through TEM imaging.[25]

The calculations by Qian et al. were performed assuming ideal vacuum conditions. Reference 26 suggests that the vacuum in the microscope used in the experiment ($\sim 9 \times 10^{-6}$ Torr) is strong enough to prevent the formation of a layer of water and/or oxygen molecules that would likely be produced at standard pressure on the surfaces of CNTs which are graphite-like. These molecules may act to satisfy the dispersive needs of the fresh surfaces as the inner bundle is pulled from the sheath, moving atoms out of the vdW registry. At least in graphite, such layers serve to catalyze the sliding process.[26] In the experimental vacuum, the energy supplied to break the dispersive bonds is not dissipated, but remains as potential energy in the system until the vacuum in the microscope is released. Thus, the results should be directly comparable to those of the theory. This dispersive energy should result in a constant force that resists inner-bundle extraction, and has been described previously in relation to the forces that act between walls of MWNTs.[21]

In the following sections, we present the results of in situ SEM pullout experiments conducted on DWNT bundles which have been used, in particular, to estimate the normalized sliding force. The results for sliding between adjacent DWNTs are presented which show that a well-defined pullout force can be measured. Subsequently we use theoretical modeling to explore the origin of the pullout force, beginning with a study of shear interactions between adjacent CNTs modeled using MM3-based molecular mechanics (MM) and density functional theory simulations.[27−29] We also consider the thermodynamics associated with making new surfaces, showing that this leads to an estimate of the force that is similar to that from the MM3 calculations, but that in both cases this force is much lower than the experimentally estimated force. The theoretical modeling also considers the effects of functional groups (OH) that decorate the surfaces of the nanotubes, carbonyl groups at the position of dangling bonds where the outer tubes are fractured, corrugation in CNT-CNT interactions, and polygonization of the CNTs arising from squeezing effects. The sum of all these potential energy effects is found to account for less than half of the experimental estimate of the force. However, a top-down analysis of dissipation based on the observed lack of reversibility of the pullout process indicates that dissipation is responsible for at least half of the pullout force, therefore the sum of potential energy and dissipation contributions gives a result within the error bars of the experiments.

■ IN SITU SEM EXPERIMENTS

Hexagonally packed bundles, composed of DWNTs each with an outer diameter of approximately 2.2 nm, were isolated from mats produced by MER Corporation. Directly from the CVD reactor, the pristine bundles are coated in a thin layer of polymer, which is thought to wrap around the outside of the bundles. To remove the polymer, a heat treatment was applied, following a previously described procedure, at temperatures of up to ~600 °C.[12] High-resolution transmission electron microscopy (HRTEM) images of the bundles revealed a tube−tube fringe spacing of 2.54 ± 0.06 nm between adjacent DWNTs. This suggests a gap spacing between adjacent DWNTs of 3.4 ± 0.6 Å, which is similar to the interlayer spacing in graphite. This implies that adjacent DWNTs interact

dx.doi.org/10.1021/nl203686d | Nano Lett. 2012, 12, 732−742

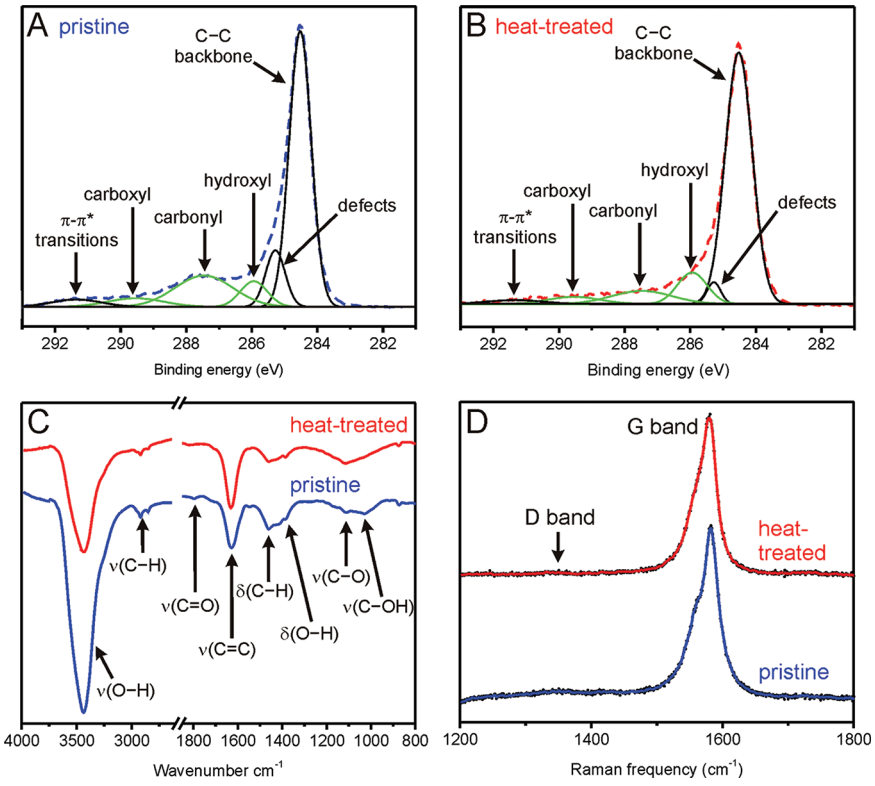

Figure 1. Deconvoluted XPS spectra in the C1s region of pristine (A) and heat-treated (B) DWNT mats. All deconvoluted signals are labeled, with those originating from oxygen-containing functional groups highlighted in green. (C) FTIR spectra of pristine and heat-treated mats with labeled stretching (υ) and bending (δ) modes. (D) Raman spectra of pristine and heat-treated mats with D and G bands labeled.

via purely vdW interactions or perhaps small functional groups that may exist on the outsides of the tubes.

X-ray photoelectron (XPS) and Fourier transform infrared (FTIR) spectra of the DWNT mats suggest removal of most of the polymer from the bundles by the heat treatment. Binding energy values in the XPS were calibrated to the location of the C═C bond signature (284.5 eV) in the CNT structure. Prior to treatment, the types and proportions of oxygen-containing functional groups, can be determined by deconvoluting the C1s XPS (Figure 1A), green lines.[30] In addition, the pristine bundles contain a signal from carbonyl groups (278.5 eV), which suggests a relatively large concentration of this functionality compared to other oxygen-containing groups. This agrees with our previous analysis of this material.[12] Weaker signals are also present in the XPS, suggesting the presence of carboxyl (289.4 eV) and hydroxyl (285.8 eV) groups. Heat treatment of the mats significantly weakens the intensity of the carbonyl signal (Figure 1B), suggesting pyrolysis of this group. The abundance of hydroxyl groups seems to be slightly increased by the heat treatment, while the concentration of carboxyl groups appears to remain constant. Thus, residual moieties seem to remain on the bundle surfaces after heating.

Because XPS spectroscopy is a technique that probes to a depth of just a few nanometers, FTIR spectroscopy was employed to investigate the possibility of removal of functional groups from inside the bundles. The presence of signals for hydroxyl (ν(O–H) and ν(C–OH)) and carbonyl (ν(C═O)) functionalities in the spectrum of the pristine DWNT bundles (Figure 2C) agrees well with the aforementioned XPS data. Also evident is the presence of alkyl groups (ν(C–H) and δ(C–H)), most likely in the form of alkyl groups on an acryloyl

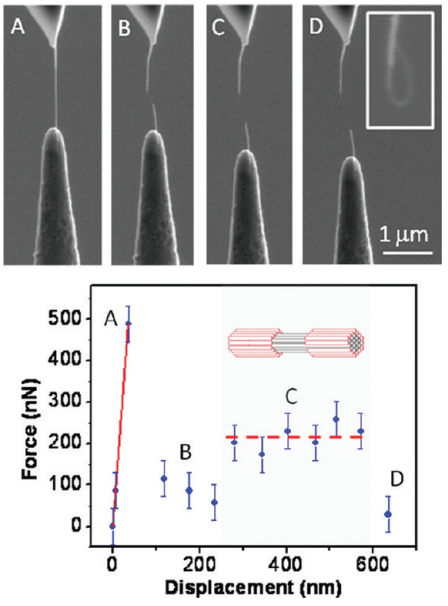

Figure 2. (Top) Sequential SEM images recorded during shear testing of an isolated bundle of DWNTs. The inset shows a smaller inner bundle which pulled out of an outer shell of DWNTs. (Bottom) Force vs displacement recorded during the pullout experiment. The labels indicate the different stages: (A) Tensioning of the original bundle, (B) restraightening after initial failure, (C) pullout of the inner bundle from the outer shell, and (D) final failure of the bundle. Error bars correspond to the force associated with one pixel in the measured deflection of the cantilever.

base, as previously reported.[12] After heat treatment, the intensity of signal originating from all of the oxygen-containing

dx.doi.org/10.1021/nl203686d | Nano Lett. 2012, 12, 732–742

functional groups decreases, while the signal from the CNT backbone (ν(C=C)) remains strong. Weak signals from the oxygen-containing groups remain in the FTIR spectrum (Figure 2C); these low intensity signals, which do not originate from the nanotube structure, confirm a decrease in the polymer layer on the exterior of the bundles. However, the residual oxygen-containing peaks provide evidence that in addition to the low density of polymer remaining on the surface, some hydroxyl and carbonyl groups may exist within the bundles. Details of differences in the FT-IR measurements of pristine and heat treated samples can be found in the Supporting Information.

As mentioned in the introduction, approaches to promoting interaction within and between DWNTs, including e-beam cross-linking, can introduce defects. Our DWNTs have very low defect densities. Indeed, the Raman spectrum (Figure 1D) of our as-fabricated mats contains a sharp G band (~1580 cm^{-1}) with a barely perceptible D band (~1350 cm^{-1}) that is indicative of a very low density of sp^3-hybridized carbon atoms. The overall structure of the CNTs was not diminished by the heat treatment, as no discernible variance in the ratio of the D and G bands could be distinguished from these spectra. This retention of structure agrees well with previous work, where evidence for the creation of new defects in DWNT bundles was only detected after heating above 2000 °C.[31] Although the XPS and FTIR data reveal residual oxygen-containing peaks after the heat treatment, they do not indicate if these remaining moieties exist on the outside or inside of the bundles. The low density of sp^3-hybridized carbon atoms revealed by Raman spectroscopy, however, suggest that only a very low density (if any) functional groups, chemically bonded to the CNTs, exist inside the bundles.

The shear interactions between heat-treated DWNTs within the bundles were investigated using an in situ scanning electron microscopy (SEM) testing setup with a Si cantilever-based force sensor described in detail previously.[12] Pullout experiments were conducted on individual bundles which measured the force as a function of sliding displacement for inner DWNTs sliding relative to an outer shell of DWNTs. During each pullout experiment, one end of the bundle was displaced by a nanomanipulator (Klocke) and the force was determined at each displacement step by measuring the deflection of the Si cantilever (with known stiffness) using cross-correlation of sequential high resolution SEM images.[12]

To investigate the shear interactions, isolated bundles were first deformed in tension until failure of the outer shell occurred, as indicated by point A in Figure 2 plot. At the point of this initial failure, a smaller inner bundle was found to partially pull out of the outer shell in a sword-in-sheath-like failure mechanism, accompanied by corresponding recoil of the cantilever-based load sensor. The difference between the diameters of the initial and pulled-out bundles was about twice the diameter of the DWNTs, suggesting the failure of just the outermost layer of tubes. The inner bundle did not retract back into the tube sheath over a period of a few seconds, despite the observed slack in the pulled-out inner bundle. Subsequent to the initial failure, one end of the bundle was then further displaced to retension the bundle (points B in Figure 2). A pullout experiment was then conducted in which the force was measured as a function of the relative sliding displacement between the inner and outer shells of DWNTs. The force was found to plateau (pullout force of ~215 nN) during sliding (points C in Figure 2) and then drop to zero upon complete pullout (point D in Figure 2). The free end of the inner bundle then snapped back and formed a loop (inset in Figure 2). Variations in the force at points where the bundle is untensioned and across the plateau region are attributed to instrumental drift during SEM imaging. It should be noted that pullout experiments were conducted over a period of several seconds at the lowest practical magnification so as to minimize any beam-induced carbon deposition on the interface of interest.

Experiments were conducted on three individual bundles. All exhibited similar force-displacement behavior to that shown in Figure 2. For each experiment, the number of tube−tube interactions at the shear interface was estimated in order to normalize the pullout force and allow a better comparison of the interactions for bundles with different diameters. A justification of this normalization method is discussed in detail in the context of results of the MM analysis in the next section. The number of tube−tube interactions, $N_{CNT\text{-}CNT}$, was estimated using a geometrical model of hexagonally packed DWNTs yielding:

$$N_{CNT-CNT} = 2N + 6$$

where N is the number of DWNTs on the perimeter of the inner bundle. N can be estimated from the diameter of the inner bundle[12] which was measured from SEM images. Results from all pullout experiments revealed similar normalized pullout forces of 1.7 ± 1.0 nN/CNT−CNT interaction. Note that the pullout force was independent of the overlap length of the inner bundle and outer sheath.

Analogous pulling experiments were also performed on bundles not subjected to the heat treatment. They were found to undergo nearly complete failure at the initial failure point (points A in Figure 2), and did not exhibit a secondary load-bearing regime (points C in Figure 2). This nearly complete failure was confirmed by TEM imaging, which revealed a fractured region with a staggered diameter, i.e., telescopic failure where multiple layers of tubes had failed. This type of failure mechanism has been previously observed for similar polymer-coated bundles.[12] It may be the result of external pressure acting on the bundles, due to the polymer coating, and will be the subject of future investigations.

THEORETICAL ANALYSIS

To understand the nature of the shear interactions between adjacent DWNTs within bundles, MM simulations of sliding between CNTs were conducted. The TINKER 5.1[32] molecular mechanics/dynamics software package and the MM3 force field[27−29] were used. MM3 is a well-known force field for modeling organic molecules that includes electrostatic and dispersion interactions as well as more subtle effects such as the interactions of charged groups with the π-cloud of an aromatic ring. To calibrate the quality of these MM results, we have also performed electronic structure calculations using the density functional tight binding with empirical dispersive corrections (DFTB-D) method[33] for a small model of the nanotube structures we have studied. Details can be found in the Supporting Information.

MM simulations with several different sliding configurations were investigated: (1) pairs and groups of three CNTs sliding with respect to one another and (2) a CNT being pulled out of six outer CNTs in a close-packed bundle. Figure 3 shows the pair- and bundle-tube arrangements. The three-tube groups consisted of a middle tube with tubes directly above and below

dx.doi.org/10.1021/nl203686d | Nano Lett. 2012, 12, 732−742

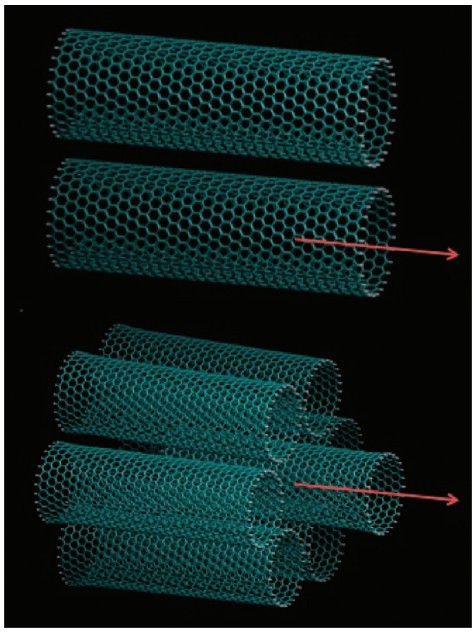

Figure 3. Configurations for (top) pairs of SWNTs (2 × CNT) and (bottom) a seven-SWNT (7 × CNT) bundle. The arrows indicate the direction of pulling applied in simulations.

it. In addition to the different sliding configurations, we investigated the shear forces for sliding in three CNT systems: (i) bare CNTs terminated with hydrogen atoms at the free edges, (ii) bare CNTs terminated with carbonyl groups at one free edge and hydrogen atoms on the remaining edges, and (iii) CNTs with hydroxyl groups on their surfaces.

The models were created as follows: (1) A single (27,0) CNT (chosen to match the outer wall diameter of the DWNTs studied in experiments) with either hydrogen- or carbonyl-terminated ends and a bare or OH-functionalized surface was geometry-optimized. Single-walled tubes were used instead of DWNTs for computational efficiency and because preliminary calculations showed that the interaction energy between the tubes was not sensitive to the presence of an inner shell. (2) The optimized CNT was duplicated and the system of parallel tubes was optimized, starting from a separation of 6 Å between the walls. (3) This minimized structure was used as the initial structure for the next minimization, in which one of the tubes in the pair, the center tube in the group of three tubes, or the middle tube in the seven-tube bundle was displaced by 0.2 Å, and the optimization was repeated. In the two-tube (2 × CNT) and three-tube (3 × CNT) simulations, the positions of the end rings of carbon atoms were fixed at one end of each tube. In the seven-tube (7 × CNT) simulations, the ends were tethered to a fixed Kr atom by a flat-well harmonic as described further in the Supporting Information. Because these systems are rigid, stepwise MM optimization along the pulling axis resulted in a small change in energy from one step to the next, allowing for the estimation of the shear force by finite difference.

Considerations of computation run times limited the number of atoms and thus the CNT lengths that could be simulated. In the experiment (shown in Figure 2), the overlap region prior to pullout was ~300 nm in length. The simulation of tubes of this length is not practical with a high-quality force field such as MM3. To investigate the effect of varying initial overlap length, and to identify the appropriate overlap for the remaining

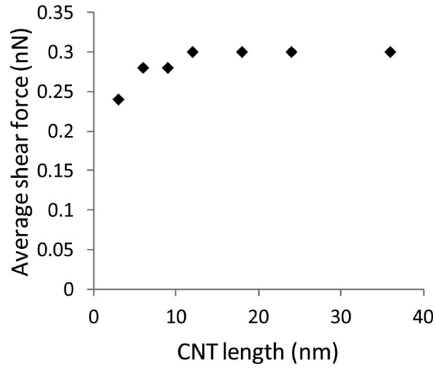

Figure 4. Shear force determined from MM simulations as a function of CNT overlap length for sliding between pairs of bare (27,0) CNTs with H atom edges.

calculations, simulations were conducted to investigate forces as a function of overlap.

I. Hydrogen-Terminated CNTs. Figure 4 shows the results of simulations in which pairs of bare H-terminated (27,0) CNTs of varying lengths (3–36 nm) were slid past one another. It is clear from this figure that the average sliding force increases with length for lengths of <12 nm. A saturation effect is observed for longer tubes. This finding is consistent with the experimental pullout tests in which the pullout force was found to be constant, as the inner bundle was pulled out of the outer shell. The MM simulations suggest that a gradual reduction in the pullout force would only occur when the overlap length in the experiment was less than ~12 nm, which is smaller than the displacement step size of the experiment. Overlap lengths of 6 nm result in < 10% underestimate of the force. Therefore, to keep computational costs manageable, the simulations were performed starting with this overlap.

Because there are many CNT–CNT interactions in the experimental bundles, we studied a range of two to six CNT–CNT interactions to investigate whether or not the pullout force is an additive interaction. Figure 5A illustrates the model and Figure 5B shows the results for 2 × CNT, 3 × CNT, and 7 × CNT H-terminated cases. As can be seen in the Figure 5B, the prediction for two interactions is approximately double that of one, and the pullout force on the central tube is approximately six times that of a single interaction; the pullout force seems to be an additive interaction.

The forces oscillate with displacement, with a periodicity that is associated with the graphitic lattice structure of the tube walls and their registry. These oscillations are discussed in more detail in subsection III. In the absence of dissipation, it is the average force (~0.3 nN/CNT–CNT interaction) that is relevant for comparison to experiment.[34] This is because the experimental sliding surfaces are large and composed of many CNTs, which will be in different positions relative to the registry, leading to an averaging of the Å-level oscillations observed in the simulations. The amplitude of the oscillations decreases as the free tube ends approach each other. This effect is a consequence of the use of short tubes in these simulations, and is only relevant when overlaps are below the ~12 nm length.

It is useful to compare the 0.3 nN estimate of the pullout force based on the MM3 calculations to the result of a thermodynamic analysis based on the potential energy that must be overcome to create new surface. Assuming complete relaxation and using 0.035 eV/atom as the amount of vdW

dx.doi.org/10.1021/nl203686d | Nano Lett. 2012, 12, 732–742

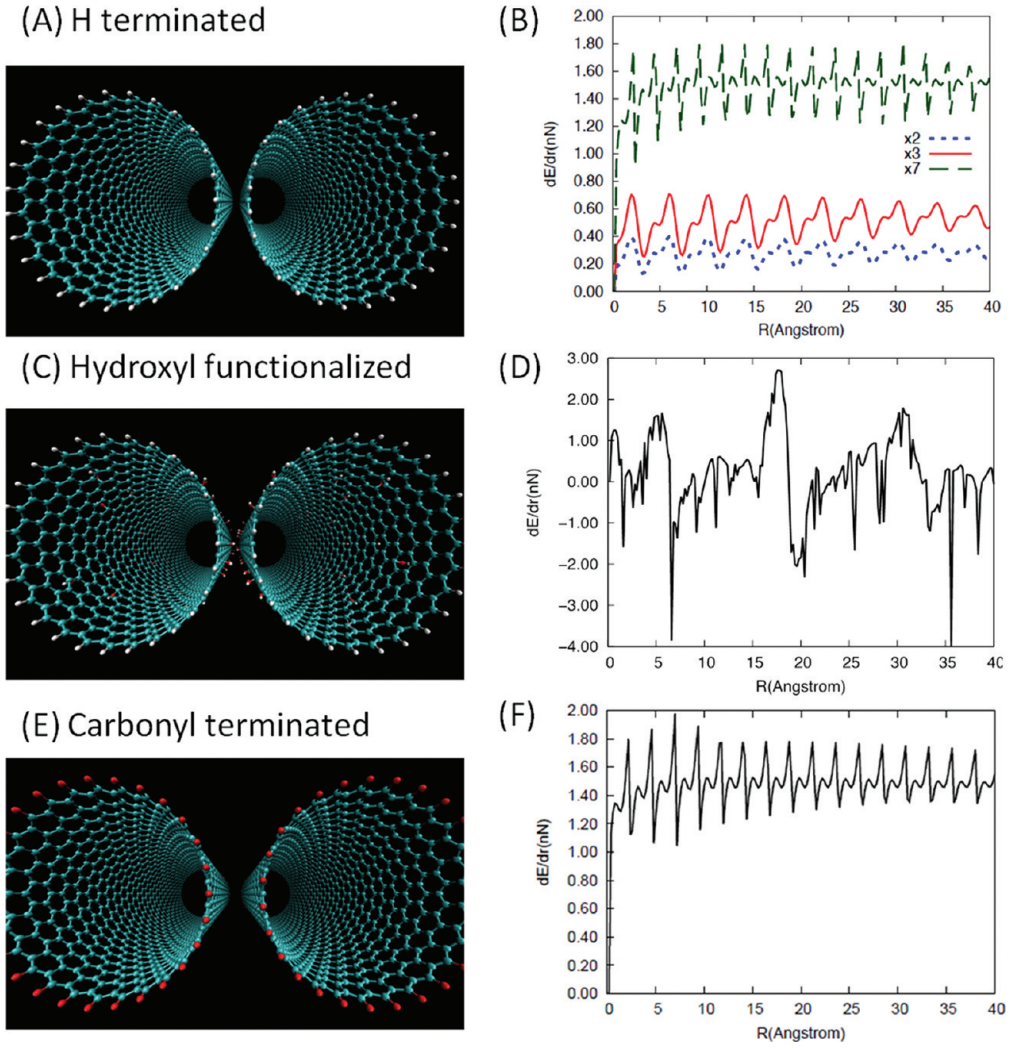

Figure 5. MM simulations of three (27,0) CNT sliding configurations. (A) MM model of hydrogen-terminated SWNTs. (B) Shear force as a function of the number of interacting 6 nm H-terminated CNTs: 2 × CNT (one interaction), 3 × CNT (two interactions), and 7 × CNT (six interactions). (C) MM model of hydroxyl-functionalized SWNTs. (D) Shear force for a 2 × CNT model with tubes functionalized with 4% OH. (E) MM model of carbonyl-terminated SWNTs. (F) Shear force on the central tube pulled out from a 7 × CNT bundle, with one end of the central tube terminated with carbonyl groups.

energy stored in graphite,[35] the force required for pullout can be estimated from the number of carbon−carbon interactions that must be broken to displace the nanotubes by 4.3 Å, the periodicity of the CNT. This gives a force of ∼0.4 nN/CNT−CNT interaction, which is similar to that obtained from the MM3 calculations. These two forces are not expected to be precisely the same, as the MM3 result refers to a pullout path that is not completely reversible (due to the finite step used in the estimate). Also, the MM3 result involves an average over oscillations, while the vdW estimate refers only to the equilibrium structure. Nevertheless, the closeness of the two numbers provides confidence that any differences between them are of minor consequence.

Since the 0.3−0.4 nN force estimates are significantly lower than the forces measured in the experiment (∼1.7 nN/CNT−CNT interaction), we infer that vdW interactions alone involving bare nanotube structures cannot explain the experimentally measured pullout force. To further investigate the nature of the shear interactions present in the experiments, MM simulations that include functional groups are discussed next.

II. Hydroxyl-Functionalized CNTs. The investigation of OH groups on the CNT surfaces was motivated by XPS and FTIR spectra which suggest that some residual oxygen containing groups are present on or within the bundles after heat treatment. The choice of short functional groups, as opposed to longer polymer cross-links, is supported by HRTEM imaging, which demonstrated a 3.4 ± 0.6 Å spacing between adjacent tubes within the bundles (similar to the spacing between layers in graphite). Using a comparison between the experimentally measured CNT−CNT spacing, and the spacing predicted from MM simulations, the possible OH density present in experiments was approximated to be up to 2−4 OH groups per 100 carbon atoms (2−4%) (see the Supporting Information for details). Figure 5C,D shows the results from MM simulations for 12 nm 2 × CNTs functionalized with 4% OH groups. The most significant peaks and valleys shown in the top panel are largely a reflection of when OH groups on one tube encounter OH groups on the other. Note that hydroxyl groups can both push and pull on one another, leading to both positive and negative forces. Interestingly, we see that the average sliding force is ∼0.13 nN/

dx.doi.org/10.1021/nl203686d | Nano Lett. 2012, 12, 732−742

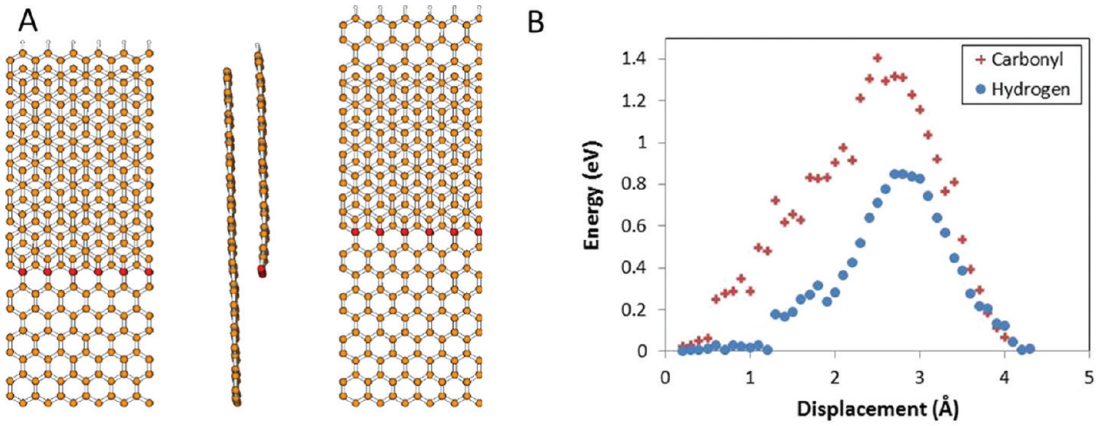

Figure 6. (A) Top and side views of the zigzag edge model. The top view of the model after the partial sheet has been displaced one periodic distance is also shown (right panel). The free edge is functionalized with carbonyl groups. Carbon, hydrogen, and oxygen atoms are shaded yellow, white, and red, respectively. (B) Energy versus displacement associated with the zigzag model with carbonyl groups or hydrogen atoms at the edge.

CNT−CNT interaction. This force is two to three times smaller than for bare tubes. This demonstrates that OH−OH interactions can actually have a lubricating effect on the interface, causing an increased separation between adjacent CNTs and effectively reducing the average sliding force by interfering with the vdW registry. This lack of evidence of OH groups within the bundles is consistent with the Raman spectra of the material, as previously discussed.

The oscillations around the average force are large (~-4 to 3 nN/CNT−CNT interaction). It is the average that is relevant to the pullout force in the absence of dissipation. However, the fluctuations about the average can contribute to dissipation. In fact, the fluctuations are so large that they could explain all of the dissipation in principle. Nonetheless, the extent of functionalization is crucial to the importance of this effect, and this is likely smaller than in the calculations. This issue will be discussed further in the Conclusion section.

III. Carbonyl-Terminated CNTs. Upon the fracture of the outer tubes of the bundle, in the first stage of the pullout experiment, dangling bonds are created. In ref 36, the authors used simulations to examine the pullout of an inner tube from a multiwalled CNT, and showed that significantly more force is necessary to extract an inner tube with an end consisting of dangling bonds than one with a fullerene-like cap. This suggests that end-effects are an important consideration for this type of problem. However, even though our experiment is performed in a vacuum of $\sim 9 \times 10^{-6}$ Torr, the diffusion rate of gas molecules on the surface is sufficiently large that the bonds are rapidly functionalized. The barrier to diffusion of O_2 is less than 3 kcal/mol.[37] When an O_2 molecule is placed near the dangling bonds of the type that are expected experimentally, density functional theory calculations based on the Perdew−Burke−Ernzerhof functional with a double-ζ plus polarization orbital basis set (PBE/DZP) suggest that it dissociates to form a pair of carbonyl groups. This observation motivated several sets of MM simulations in which a SWNT with an end terminated with carbonyl groups was pulled out of a seven-tube bundle. Figure 5E,F shows the results of these simulations, which suggests nearly the same force as for the fully hydrogen-terminated tube bundle.

To further investigate the effect of carbonyl functionalites, these groups were added to zigzag and armchair edges of graphene sheets, and then moved across intact sheets of graphene in PBE/DZP-based simulations. The zigzag model is shown in Figure 6A. Periodic boundary conditions were used, and hydrogen atoms were used to terminate what would otherwise be dangling bonds. The armchair model is analogous (not shown). The partial sheets were moved one periodic distance, i.e., 4.3 and 2.5 Å, for the models of the zigzag and armchair edges, respectively. A 0.1 Å step size was used and the positions of all but the hydrogen atom on the partial sheet and the row of carbon atoms at the opposite end of the full sheet were optimized. The resulting energy versus displacement behavior for the zigzag model is shown in Figure 6B. The interaction is a combination of the dipole−induced dipole interactions between the carbonyl groups and the neighboring sheet, and the dispersive interactions between the carbon atoms of the adjacent graphene sheets. Note that no new surface is created by the displacements in these calculations.

It is well-known that density functional theory is generally unable to accurately predict the energy and thus the forces due to dispersion. Therefore, calculations were repeated in which the O atoms were replaced by hydrogen atoms. In this latter set of calculations, all atomic positions were fixed at the corresponding optimized values found in the calculations in which the carbonyls were included, except for those of the newly added hydrogen atoms. The resulting energy versus displacement behavior for the zigzag edge model is also shown in Figure 6B. By subtracting off the contribution from graphene-graphene interactions in the absence of carbonyl groups (1.4 − 0.85 = 0.55 eV), and using the fact that this energy change takes place over a pullout distance of approximately 4.3 Å, this gives a force of 0.128 eV/Å or $1100 \times 2 \times 0.128/14.8 = 19.0$ eV/Å at the bundle level, where an inner bundle circumference of $25 \times 14\pi = 1100$ Å has been assumed. The width of the unit cell used in the PBE/DZP calculations is 14.8 Å. The factor of 2 comes from the fact that two such carbonyl-functionalized ends will be moving over the surfaces of intact tubes as the pullout takes place. This translates to a force of 30.4 nN at the bundle level (0.24 nN/CNT−CNT interaction).

The force was calculated as the average slope of the energy versus displacement curve between the position of the energy minimum and energy maximum, and was then averaged over the full periodic displacement.[38] The energy released as the carbonyl groups pass over the energy maximum will likely be dissipated. Interestingly, the addition of carbonyls to the armchair edge (not shown) did not increase the resistance to

dx.doi.org/10.1021/nl203686d | Nano Lett. 2012, 12, 732−742

sliding beyond that due to graphene-graphene interactions in the absence of carbonyls.

The 30.4 nN force for zigzag graphene corresponds to a graphene-graphene interaction, and thus must be multiplied by a factor less than one to take into account the curvature of the tubes. The SWNT models of ref 23 suggest that a factor as large as 0.6 might be appropriate, a result that is consistent with the SWNT models of ref 39. However, the fact that our experimental tubes are double-walled, and thus significantly less prone to radial deformation than SWNTs,[39] and that our more sophisticated force field suggests that SWNTs are less prone to such deformations than the fields used in refs 23 and 39 (see next section) suggest that a smaller value might be appropriate. Regardless, even the use of the 0.6 multiplication factor gives a force of less than 20 nN at the bundle level (0.16 nN/CNT-CNT interaction), i.e., the carbonyl groups only lead to a small contribution to the force resisting pullout, in agreement with the MM3 result.

IV. Corrugation Effects. In Figure 5B,F, force oscillations, which are caused by the corrugation potential associated with the vdW registry, take place around an average force that is associated with the vdW energy necessary to create new surfaces. This type of oscillation can cause stick−slip motion.[38] However, what will be measured experimentally in our system is the average of the force that resists the applied strain.[34] The averaging occurs because the experimental surfaces are large and the loading of junctions (contact points) will be uneven on the Å length-scale.[34]

The forces associated with the negative part of the oscillations will not be measured experimentally, whereas in vdW registry, the atoms exert no net forces on each other. As they are forced out of registry by the testing equipment, atoms get closer to and/or further from each other than they were while in the registry, i.e., they are subjected to net local attractive or repulsive forces. When a local energy inflection point is passed, this will result in vibrations, i.e., dissipation, no matter how slowly the pullout occurs. Note that the pullout rate is very slow ($\sim 1 \times 10^{-13}$ Å/fs), so some energy may be coupled into pushing on the tubes as corrugation energy inflection points are passed. Nevertheless, loading of the various junctions will be uneven, a situation that will lead to dissipation.[34]

The interpretation of the pullout force is an extension of eq 1 in ref 21. It is also in the spirit of the Tomlinson model of friction.[40] For the (27,0) tubes used in the simulations, the corrugation potential has a wavevector of $c = 2\pi/a$, where a = 4.3 Å. In the 7 × CNT cases (in which atom tethers were used), rotation of the tubes around their long axes was observed, complicating the oscillatory behavior of the force. Other tube chiralities are associated with different periodicities, e.g., (n,n) tubes have a periodicity of 2.5 Å The amplitude of the oscillations are a function of the chirality of the tubes in the bundle, and reflects how effectively the tubes access the vdW registry.[41]

The amplitude of the oscillations associated with the corrugation potential shows a weak dependence on the amount of overlap between the tubes. Tubes sliding by one another that are strained by different amounts, or strained in the opposite direction, have hexagonal rings that will only have a limited region of overlap that will produce an energy minimum. Similarly, in a DWCNT, when the walls do not effectively access the registry, friction between them is small, and it can be independent of the amount of overlap.[42] Note that the difference in energy between the maximum and minimum energies associated with the registry is small compared to the amount of vdW energy associated with bringing two tubes close to their optimal vdW separation.[43]

V. Polygonization. As the bundles form, the tendency of the tubes to enter vdW registry will cause them to polygonize (i.e., to distort into hexagonal shapes). This will result in bond bending and bond length changes, leading to a change in the potential energy of interaction between the CNTs. As the pullout occurs, these bond angle and length changes will relax as the possibility of vdW interactions between tubes is reduced. In principle, the associated energy could be dissipated.

As one estimate of the magnitude of this effect, the amount of energy stored in bending and length changes was estimated using MM3 for a 7 x SWNT bundle, 12 nm in length, by (1) optimizing the geometry of the bundle, (2) fixing the geometry of the inner tube, (3) removing the outer six tubes, (4) calculating the energy of the inner tube, which had been "squeezed" by the other six DWNTs (this squeezing energy is labeled E_{sq}), and (5) geometry optimizing this tube and calculating its relaxed energy, E_{re}. $E_{sq} - E_{re}$ is the amount of energy stored in bond length and angle changes, in the inner tube. MM3 simulations suggest that this energy difference is 1.36 eV per 12 nm, which translates to a force of 0.02 nN/CNT−CNT interaction if all of this potential energy is dissipated. Therefore, according to MM3, this is not an important dissipation source.

The MM3 simulations thus suggest that the tubes have quite rigid cross sections. Other simulations suggest that they may be significantly more flexible.[23,39] For example, the MM simulations in ref 39 suggest that 2.2 nm DWNTs polygonize by ∼20% when in a bundle. Therefore, it is useful to have an upper bound on the amount of energy that can be stored in length and angle changes. This value cannot exceed the amount of vdW energy that could be gained from the complete relaxation of the tubes against each other, thus, effectively forming a pair of curved graphite layers. This is because it is the vdW force that causes the bending and length changes. In section I, we estimated this vdW force as ∼0.4 nN/CNT−CNT interaction based on 0.035 eV/atom as the amount of vdW energy stored in graphite.[35] Using this estimate, ref 39 suggests that up to ∼0.08 nN/CNT−CNT interaction (20% of 0.4 nN) may be due to this form of dissipation.

VI. Top-down Estimate of Dissipation Effects. The potential energy effects described in the preceding section can all contribute to dissipation, as we have already argued in the case of the corrugation and polygonization energies. The fact that the inner bundle does not pull back into the sheath after the outer tubes are broken allows for the establishment of a lower bound on the total amount of dissipation, as we will discuss in the following paragraphs.

The force applied to pull out the inner bundle after the outer sheath is broken can be represented by

$$F = F_p + F_{dd}$$

where F_p is the force due to an increase in potential energy of the system and F_{dd} is the "dynamic dissipation" force due to dissipation caused by dynamic friction. From the measurements, we know that $F_p + F_{dd} \sim 215$ nN, but the magnitude of either force is unknown.

If the inner bundle were to be released during pullout or equivalently when it is necessary to apply force to straighten the inner bundle, $F = 0$ at the point where the inner bundle meets the edge of the sheath. F_p is the same as it was during the

dx.doi.org/10.1021/nl203686d | Nano Lett. 2012, 12, 732−742

Table 1. Summary of the Various Contributions to the ~1.7 nN/CNT−CNT Interaction Pullout Force[a]

contribution	dissipation	surface energy	carbonyl groups	corrugation	polygonization
force (nN)	>0.85	≤0.4	≤0.16	~0.1	~0.02−0.08

[a]Estimates of the contribution due to total dissipation, the energy necessary to create new vdW surfaces, the contribution due to carbonyl end groups, the corrugation potential associated with the vdW registry, and the energy stored in bond length and angle changes as vdW forces squeeze the tubes together (polygonization) are provided. Units are nN/CNT−CNT interaction.

pullout. It is a static friction force, F_s, that keeps the bundle from moving back into the sheath, which means that

$$F_p + F_s = 0$$

F_s must be less than the maximum static friction force the material can exert, F_{sm}. Now, because of the surface structure of CNTs and because the pullout is very slow, it is not expected that the area of real contact between the sheath and the inner bundle will be much different under static versus dynamic conditions. As such

$$|F_{sm}| \approx |F_{dd}|$$

and thus

$$|F_{dd}| > |F_p|$$

which means that at least half of the 215 nN (1.7 nN/CNT-CNT interaction) is due to dissipation. In other words, F_{dd} > 0.85 nN. Note that this assumes F_{dd} is independent of direction. It should be noted that this analysis does not identify the origin of the dissipation (and that is why we have described it as a "top-down" estimate).

VII. Summary of Theoretical Results. Table 1 summarizes the various contributions to the pullout force that we have estimated. Note that we have chosen to use the 0.4 nN estimate of the vdW energy rather than 0.3 nN force estimated from the MM3 calculation. Also note that the surface force, force from carbonyl groups, corrugation force, and polygonization force have been calculated using potential energy changes, but would also contribute to the dissipative force based on the reversibility arguments given above. This analysis shows that the sum of force components excluding dissipation is on the order of 0.7 nN (half of the pullout force, within the experimental error bars). Therefore the sum of this plus dissipation (>1.55 nN) is consistent with the 1.7 ± 1.0 nN experimentally measured force within experimental error.

CONCLUSIONS

In situ SEM experiments were conducted to measure the force required to pull out an inner bundle of DWNTs from a larger outer bundle. A sword-in-sheath-type failure mechanism was observed. These experiments allowed for a quantitative determination of the shear forces acting between adjacent DWNTs within a bundle. The forces were measured to be 1.7 ± 1.0 nN/CNT−CNT interaction and were found to be independent of overlap length over the range of displacements applied in the tests. MM and PBE/DZP simulations of both bare and functionalized CNTs were conducted to provide insight into the nature of the shear interactions. Simulations of sliding between bare H-terminated tubes, for which only vdW interactions between adjacent CNT shells are relevant, predicted lower forces (~0.3 nN/CNT−CNT interaction) than those observed experimentally. This estimate of the force was found to be similar to what can be estimated from the energy required to produce new surfaces (0.4 nN/CNT−CNT interaction). MM simulations of CNTs with a low density of OH functional groups (4 OH groups per 100 C atoms), for which a sliding force of ~0.13 nN/CNT−CNT interaction was predicted, suggest that hydroxyl groups at this concentration would have a lubricating effect were they to be present on the tubes in the experiments. This effect was attributed to the separation of adjacent CNTs, which disrupts the vdW registry, and a push−pull mechanism between interacting OH groups. Although there could be considerable dissipation associated with this mechanism, the Raman spectra suggest that OH or other groups are unlikely to be present between tubes in the experiments. The presence of a sufficient concentration of oxygen molecules within the SEM chamber during the pullout, combined with PBE/DZP-based simulations, suggests that the dangling bonds created during the fracture of the outer tubes will quickly become functionalized with carbonyl groups. MM and PBE/DZP simulations suggest that these carbonyls may make a minor contribution (0.16 nN/CNT−CNT interaction) to the force required for pullout. Other small contributions are associated with corrugation in the CNT−CNT interaction (~0.1 nN), and from polygonization of the CNTs (0.02−0.08 nN).

On the basis of the experimental observation that the inner bundle does not pull itself back into the sheath, we have argued that dissipation is responsible for at least half of the inner bundle pullout force. This is consistent with our estimate of 0.7 nN as the sum of the potential energy contributions to the pullout force, which is half the measured force within the uncertainty of the measurement. Much of the dissipation can be associated with the effects we have studied, as every component of the potential energy can be matched by dissipation based on the reversibility argument. However, this argument does not tell us the detailed mechanisms of dissipation. While this high dissipation result is in contrast to the work of Cummings and Zettl,[21] who found very low dissipation effects in the pullout experiments associated with MWNTs, these are physically different systems so agreement is not expected. Nevertheless these findings suggest that the bundle hierarchical level within CNT yarns may play a crucial role in the energy dissipation capabilities of yarns. Finally, we note that although the mechanisms of dissipation are not fully revealed based on our structural models, we have developed a meaningful interpretation of the measurements.

There are many processes that we did not consider that may contribute to dissipation in this system. For example, the DWNTs may have important kinks and bends that require straightening before the inner bundle can be further extracted. The possibility of twisting of the tubes is relevant, because if there is enough twist, there can be irreversible behavior. Another possibility is that the external pressure provided by the residual polymer coat is strong enough that the tubes have many regions where the walls are partially collapsed.[44] Modeling the discussed contributions to dissipation would require some form of molecular dynamics calculations, as well as structural information that goes beyond what is currently

dx.doi.org/10.1021/nl203686d | Nano Lett. 2012, 12, 732−742

available. We note that this type of calculation has been done for reasonably closely related system, but only for relatively short time simulations.[45] The large size of our experimental system size and the long time scale of the pullout make such simulations computationally impractical. Dissipation in our system is likely to take place by way of low-frequency phonons,[34] which would take prohibitively large system sizes and simulation times to model accurately.

■ ASSOCIATED CONTENT

Supporting Information

Section S1 shows the method used to estimate the appropriate OH concentration for MM simulations. Section S2 summarizes the methods used to constrain the positions of the CNT ends during the pullout of a central tube from a seven-tube bundle in MM simulations. Section S3 summarizes a comparison to DFTB calculations used to validate the MM3 calculations. Section S4 shows a plot of the difference between the FT-IR spectra for pristine and heat-treated DWNT samples. This material is available free of charge via the Internet at http://pubs.acs.org.

■ AUTHOR INFORMATION

Corresponding Author

*E-mail: espinosa@northwestern.edu. Phone: (847) 467-5989. Fax (847) 491-3915.

■ ACKNOWLEDGMENTS

The authors gratefully acknowledge support from ARO through MURI award No. W911NF-09-1-0541. H.D.E. acknowledges support from ONR through award No. N00014-08-1-0108. O.C.C. was an NSF-ACC fellow (award No. CHE-0936924). The authors thank Dr. A. Moravsky of MER Corp. for synthesis of the DWNT bundles. The authors also acknowledge Dr. S. Li. of the Electron Probe Instrumentation Center (EPIC) at Northwestern for TEM imaging of DWNT bundles.

■ REFERENCES

(1) Peng, B.; Locascio, M.; Zapol, P.; Li, S.; Mielke, S. L.; Schatz, G. C.; Espinosa, H. D. Measurements of near-ultimate strength for multiwalled carbon nanotubes and irradiation-induced crosslinking improvements. *Nat. Nanotechnol.* **2008**, *3* (10), 626−631.

(2) Treacy, M. M. J.; Ebbesen, T. W.; Gibson, J. M. Exceptionally high Young's modulus observed for individual carbon nanotubes. *Nature* **1996**, *381* (6584), 678−680.

(3) Yu, M. F.; Lourie, O.; Dyer, M. J.; Moloni, K.; Kelly, T. F.; Ruoff, R. S. Strength and breaking mechanism of multiwalled carbon nanotubes under tensile load. *Science* **2000**, *287* (5453), 637−640.

(4) Yu, M. F.; Files, B. S.; Arepalli, S.; Ruoff, R. S. Tensile loading of ropes of single wall carbon nanotubes and their mechanical properties. *Phys. Rev. Lett.* **2000**, *84* (24), 5552−5555.

(5) Miaudet, P.; Badaire, S.; Maugey, M.; Derre, A.; Pichot, V.; Launois, P.; Poulin, P.; Zakri, C. Hot-drawing of single and multiwall carbon nanotube fibers for high toughness and alignment. *Nano Lett.* **2005**, *5* (11), 2212−2215.

(6) Hwang, G. L.; Shieh, Y. T.; Hwang, K. C. Efficient load transfer to polymer-grafted multiwalled carbon nanotubes in polymer composites. *Adv. Funct. Mater.* **2004**, *14* (5), 487−491.

(7) Zhang, X. F.; Liu, T.; Sreekumar, T. V.; Kumar, S.; Moore, V. C.; Hauge, R. H.; Smalley, R. E. Poly(vinyl alcohol)/SWNT composite film. *Nano Lett.* **2003**, *3* (9), 1285−1288.

(8) Dalton, A. B.; Collins, S.; Munoz, E.; Razal, J. M.; Ebron, V. H.; Ferraris, J. P.; Coleman, J. N.; Kim, B. G.; Baughman, R. H. Super-Tough carbon-nanotube fibres-these extraordinary composite fibres can be woven into electronic textiles. *Nature* **2003**, *423* (6941), 703−706.

(9) Spitalsky, Z.; Tasis, D.; Papagelis, K.; Galiotis, C. Carbon nanotube-polymer composites: chemistry, processing, mechanical and electrical properties. *Prog. Polym. Sci.* **2010**, *35* (3), 357−401.

(10) Li, Y. J.; Shimizu, H. Toward a stretchable, elastic, and electrically conductive nanocomposite: morphology and properties of poly[styrene-b-(ethylene-co-butylene)-bstyrene]/ multiwalled carbon nanotube composites fabricated by highshear processing. *Macromolecules* **2009**, *42* (7), 2587−2593.

(11) Sahoo, N. G.; Cheng, H. K. F.; Cai, J. W.; Li, L.; Chan, S. H.; Zhao, J. H.; Yu, S. Z. Improvement of mechanical and thermal properties of carbon nanotube composites through nanotube functionalization and processing methods. *Mater. Chem. Phys.* **2009**, *117* (1), 313−320.

(12) Naraghi, M.; Filleter, T.; Moravsky, A.; Locascio, M.; Loutfy, R. O.; Espinosa, H. D. A multiscale study of high performance double-walled nanotube-polymer fibers. *ACS Nano* **2010**, *4* (11), 6463−76.

(13) Filleter, T.; Bernal, R.; Li, S.; Espinosa, H. D. Ultrahigh strength and stiffness in cross-linked hierarchical carbon nanotube bundles. *Adv. Mater.* **2011**, *23*, 2855−2860.

(14) Kis, A.; Csanyi, G.; Salvetat, J. P.; Lee, T. N.; Couteau, E.; Kulik, A. J.; Benoit, W.; Brugger, J.; Forro, L. Reinforcement of single-walled carbon nanotube bundles by intertube bridging. *Nat. Mater.* **2004**, *3* (3), 153−157.

(15) Urita, K.; Suenaga, K.; Sugai, T.; Shinohara, H.; Iijima, S. In situ observation of thermal relaxation of interstitial-vacancy pair defects in a graphite gap. *Phys. Rev. Lett.* **2005**, *94* (15), 155502.

(16) Koval'chuk, A. A.; Shevchenko, V. G.; Shchegolikhin, A. N.; Nedorezova, P. M.; Klyamkina, A. N.; Aladyshev, A. M. Effect of carbon nanotube functionalization on the structural and mechanical properties of polypropylene/MWCNT composites. *Macromolecules* **2008**, *41* (20), 7536−7542.

(17) Cao, X. D.; Dong, H.; Li, C. M.; Lucia, L. A. The enhanced mechanical properties of a covalently bound chitosanmultiwalled carbon nanotube nanocomposite. *J. Appl. Polym. Sci.* **2009**, *113* (1), 466−472.

(18) Wang, W.; Ciselli, P.; Kuznetsov, E.; Peijs, T.; Barber, A. H. Effective reinforcement in carbon nanotube - polymer composites. *Philos. Trans. R. Soc. A* **2008**, *366* (1870), 1613−1626.

(19) Koziol, K.; Vilatela, J.; Moisala, A.; Motta, M.; Cunniff, P.; Sennett, M.; Windle, A. High-performance carbon nanotube fiber. *Science* **2007**, *318* (5858), 1892−1895.

(20) Motta, M.; Moisala, A.; Kinloch, I. A.; Windle, A. H. High performance fibres from 'dog bone' carbon nanotubes. *Adv. Mater.* **2007**, *19*, 3721−3726.

(21) Cumings, J.; Zettl, A. Low-friction nanoscale linear bearing realized from multiwall carbon nanotubes. *Science* **2000**, *289* (5479), 602−604.

(22) Ruoff, R. S.; Yu, M. F.; Yakobson, B. I. Controlled sliding and pullout of nested shells in individual multiwalled carbon nanotubes. *J. Phys. Chem. B* **2000**, *104* (37), 8764−8767.

(23) Qian, D.; Liu, W. K.; Ruoff, R. S. Load transfer mechanism in carbon nanotube ropes. *Composites Sci. Technol.* **2003**, *63* (11), 1561−1569.

(24) Ruoff, R. S.; Tersoff, J.; Lorents, D. C.; Subramoney, S.; Chan, B. Radial deformation of carbon nanotubes by van-der-waals forces. *Nature* **1993**, *364* (6437), 514−516.

(25) Abrams, Z. R.; Hanein, Y. Radial deformation measurements of isolated pairs of single-walled carbon nanotubes. *Carbon* **2007**, *45* (4), 738−743.

(26) Savage, R. H. Graphite lubrication. *J. Appl. Phys.* **1948**, *19* (1), 1−10.

(27) All parameters in this file are from the "MM3 PARAMETERS (2000)", as provided by Prof. Allinger, N. L., University of Georgia.

(28) Lii, J.-H.; Allinger, N. L. Directional hydrogen bonding in the MM3 force field. II. *J. Comput. Chem.* **1998**, *19*, 1001−1016.

(29) Lii, J.-H.; Allinger, N. L. Directional hydrogen bonding in the MM3 force field. I. *J. Phys. Org. Chem.* **1994**, *7*, 591−609.

(30) Datsyuk, V.; Kalyva, M.; Papagelis, K.; Parthenios, J.; Tasis, D.; Siokou, A.; Kallitsis, I.; Galiotis, C. Chemical oxidation of multiwalled carbon nanotubes. *Carbon* **2008**, *46* (6), 833−840.
(31) Kim, Y. A.; Muramatsu, H.; Hayashi, T.; Endo, M.; Terrones, M.; Dresselhaus, M. S. Thermal stability and structural changes of double-walled carbon nanotubes by heat treatment. *Chem. Phys. Lett.* **2004**, *398* (1−3), 87−92.
(32) http://dasher.wustl.edu/tinkerwiki/index.php/Main_Page.
(33) Elstner, M.; Hobza, P.; Frauenheim, T.; Suhai, S.; Kaxiras, E. Hydrogen bonding and stacking interactions of nucleic acid base pairs: a density-functional-theory based treatment. *J. Chem. Phys.* **2001**, *114* (12), 5149−5155.
(34) Persson, B. N. J., *Sliding friction: physical principles and applications*. 2nd ed.; Springer: New York, 2000.
(35) Benedict, L. X.; Chopra, N. G.; Cohen, M. L.; Zettl, A.; Louie, S. G.; Crespi, V. H. Microscopic determination of the interlayer binding energy in graphite. *Chem. Phys. Lett.* **1998**, *286* (5−6), 490−496.
(36) Xia, Z.; Curtin, W. A. Pullout forces and friction in multiwall carbon nanotubes. *Phys. Rev. B* **2004**, *69* (23), 233408.
(37) Sorescu, D. C.; Jordan, K. D.; Avouris, P. Theoretical study of oxygen adsorption on graphite and the (8,0) single-walled carbon nanotube. *J. Phys. Chem. B* **2001**, *105* (45), 11227−11232.
(38) Persson, B. N. J. Sliding friction. *Surf. Sci. Rep.* **1999**, *33* (3), 85−119.
(39) Vilatela, J. J.; Elliott, J. A.; Windle, A. H. A model for the strength of yarn-like carbon nanotube fibers. *ACS Nano* **2011**, *5* (3), 1921−1927.
(40) Tomlinson, G. A. A molecular theory of friction. *Philos. Mag.* **1929**, *7* (46), 905−939.
(41) Dienwiebel, M.; Verhoeven, G. S.; Pradeep, N.; Frenken, J. W. M.; Heimberg, J. A.; Zandbergen, H. W. Superlubricity of graphite. *Phys. Rev. Lett.* **2004**, *92* (12), 126101.
(42) Koslowski, B.; Strobel, S.; Herzog, T.; Heinz, B.; Boyen, H. G.; Notz, R.; Ziemann, P.; Spatz, J. P.; Moller, M. Fabrication of regularly arranged nanocolumns on diamond(100) using micellar masks. *J. Appl. Phys.* **2000**, *87* (10), 7533−7538.
(43) Carlson, A.; Dumitrica, T. Extended tight-binding potential for modelling intertube interactions in carbon nanotubes. *Nanotechnology* **2007**, *18* (6), 065706.
(44) Li, Q. W.; Zhang, X. H. Enhancement of friction between carbon nanotubes: an efficient strategy to strengthen fibers. *ACS Nano* **2010**, *4* (1), 312−316.
(45) Zhang, S. L.; Liu, W. K.; Ruoff, R. S. Atomistic simulations of double-walled carbon nanotubes (DWCNTs) as rotational bearings. *Nano Lett.* **2004**, *4* (2), 293−297.